NASA TECHNICAL MEMORANDUM

NASA TM X-52811

NASA TM X-52811

REDUCTION OF ALTERNATOR APPARENT-POWER REQUIREMENTS AND HARMONIC DISTORTION CAUSED BY PHASE-CONTROLLED PARASITIC LOADS

Leonard J. Gilbert and Dennis A. Perz
Lewis Research Center
Cleveland, Ohio

TECHNICAL PAPER proposed for presentation at
Fifth Intersociety Energy Conversion Engineering Conference
sponsored by the American Institute of Aeronautics and Astronautics
Las Vegas, Nevada, September 21-24, 1970

REDUCTION OF ALTERNATOR APPARENT-POWER REQUIREMENTS AND HARMONIC DISTORTION CAUSED BY PHASE-CONTROLLED PARASITIC LOADS

Leonard J. Gilbert and Dennis A. Perz

Lewis Research Center
Cleveland, Ohio

TECHNICAL PAPER proposed for presentation at

Fifth Intersociety Energy Conversion Engineering Conference
sponsored by the American Institute of Aeronautics and Astronautics
Las Vegas, Nevada, September 21-24, 1970

NATIONAL AERONAUTICS AND SPACE ADMINISTRATION

REDUCTION OF ALTERNATOR APPARENT-POWER REQUIREMENTS AND HARMONIC DISTORTION CAUSED BY PHASE-CONTROLLED PARASITIC LOADS

Leonard J. Gilbert and Dennis A. Perz
Lewis Research Center
National Aeronautics and Space Administration
Cleveland, Ohio

Abstract

The loading effect on an alternator as a result of using phase-controlled parasitic loads is shown by analysis and by test results. Because of their nonsinusoidal nature, phase-controlled parasitic load currents increase alternator apparent power (volt-ampere) requirements and introduce harmonic currents. The analysis reveals the extent to which subdividing the parasitic load reduces these unwanted effects. Test results confirm very well the reduction in apparent-power predicted by analysis. Test results also confirm the predicted reduction in load-current harmonics with parasitic load subdivision. The agreement between analytical and experimental results with respect to harmonic content, however, is limited by test circuit parameters not included in the theoretical analysis.

Introduction

The use of static phase-controlled parasitic loading in order to maintain constant power loading of a turboalternator introduces undesirable effects into the electrical system (Refs. 1 and 2). The chief undesirable effects are (1) the occurrence of nonsinusoidal currents, and (2) an increase in the alternator apparent-power (volt-ampere) requirement above that necessary to supply the maximum specified load. However, to control the turbine input power of a closed-cycle power system, the energy control and the flow of the working fluid through the turbine must be regulated. To avoid the complexity of the necessary flow controls, parasitic loading is used for power control of advanced turboalternator systems for space auxiliary electric power applications (e.g., Brayton Power Systems and SNAP-8, Refs. 3 and 4). The advantages of phase-controlled parasitic loading outweigh its shortcomings. Therefore, a better understanding of its performance is desirable. In these systems a variable electrical load (herein termed the "parasitic" load) is used in parallel with the vehicle electrical load (herein termed the "useful" load). As the demands of the vehicle useful load vary, sensing circuits provide for the adjustment of the parasitic load to complement the useful load, thereby keeping the total electrical load constant.

This paper presents a steady-state analysis of one aspect of parasitic loading. In particular, it describes the manner in which the reactive loading of the alternator varies and the extent to which harmonics occur in the alternator current when parasitic load-compensation is phase-controlled.

In order to determine the validity of the mathematical analysis, a comparison was made between the analytical results and the data from experimental hardware tests. The results of a test program performed by NASA on a 400-hertz Brayton cycle system turboalternator and its associated controls were used for comparison. This comparison indicated the accuracy and the limitations of the mathematical analysis.

This evaluation of the effects of phase-controlled parasitic loads is necessary for the proper design of turboalternator systems because apparent-power requirements determine alternator size and because nonsinusoidal currents contribute to the distortion of the generated voltage.

I. Description of Parasitic Type Speed Controllers

A. Purpose of Parasitic Loading

Figure 1 is a block diagram of a generating system typical of a parasitically loaded turboalternator system. The total load on the alternator has been divided into two electrical loads: a useful load which includes all the electrical equipments which are necessary for the performance of the mission to which the generating system is assigned, including components for the operation of the turboalternator; and a parasitic load which has been added only to control the total loading on the generating system.

When the turboalternator system is operating, the parasitic load must complement the useful load in such a manner that the combination of these loads is a constant power load on the generating system.

$$P_G = P_U + P_P \tag{1}$$

The loading system functions in the following manner: the amount of parasitic loading depends on the turbine speed (alternator electrical frequency). After the turboalternator and its load have attained a steady-state condition, any variation of the useful load changes the torque load on the turbine, which thereupon changes speed. This speed change is sensed by the parasitic-load control circuitry, and a compensating parasitic electrical load is applied to the alternator to produce an opposing speed change of the turbine. The sensitivity of the parasitic-load control circuitry is high enough so that the arrangement serves as a speed control.

With constant power load and constant speed, the driving torque of the turbine can be kept constant. As a consequence, the energy source and turbine controls are considerably simplified from what they would be if the turbine torque were varied to accommodate changing useful load.

B. Phase Control

The control of the parasitic loading described in this paper is considered to be performed completely electrically (in contrast to the use of electromechanical components such as variable transformers or resistance potentiometers). Electrical phase control of magnetic amplifier, controlled rectifier, or saturable reactor currents is the most convenient means of obtaining the necessary control of electrical power.

The term "phase control" describes the action whereby the current through a device such as a controlled rectifier can be started at any selected time (electrical firing angle) during a half cycle of the applied voltage. When phase-controlled devices are used back-to-back electrically, full-wave control is available. The electronic and magnetic devices used to effect phase control of the current in parasitic-loading systems permit totally electrical control of the parasitic-load currents, but in the process they generate nonsinusoidal periodic load currents.

II. Analysis and Discussion of Mathematical Model

A. Model

Figure 2 is a schematic diagram of the mathematical model circuit which is analyzed in this paper. The electrical power source is ideal and supplies power to two types of load: the useful load and the N parasitic loads. The parasitic loads consist of N parallel, full-wave, phase-controlled loads, each with its own control circuitry. The control of the function performed by the indicated switches is in practice performed by frequency sensitive logic circuitry. The loading component is a resistor; however, it is shown as a variable resistance-inductance combination because (as is demonstrated in the analysis which follows) the effective impedance of the phase-controlled parasitic load has such a characteristic.

The current, and therefore the power, in each parasitic-load resistor varies continuously from fully off to fully on as the electrical frequency varies over the complete range for which that branch of the total parasitic load is sensitive. For the mathematical analysis only one parasitic load (or branch) is phase-controlled at any given time. The frequency ranges of the N branches do not overlap. The loads are switched on and off sequentially.

The distribution of power between the useful load and the parasitic load is indicated diagrammatically in Fig. 3. This figure also illustrates how this parasitic load scheme serves as a frequency control. The frequency excursion from full useful load to zero useful load can be limited to any desired (and practical) range by design of the parasitic-load control.

B. Limitations of Analysis

The limiting conditions which were imposed on the mathematical model to simplify the analysis are as follows:

(1) The power source is ideal: the internal impedance is zero, and the output voltage is sinusoidal with a constant amplitude. Also, these characteristics do not change in the frequency range being considered.

(2) It is assumed that the rise time of the phase-controlled current is zero.

(3) The firing angle of the parasitic-load current is assumed to vary from 0^{o} to 180^{o}. A conduction interval of 180^{o} is attainable. There is no overlap or dead time between the frequency ranges of consecutively applied parasitic loads.

(4) The useful load consists of linear resistances and reactances.

(5) The analysis is presented for a single-phase circuit, but is also applicable to three-phase circuits if the electrical quantities are considered phase quantities.

C. Analytical Expression for Total Harmonic Distortion

Total harmonic distortion. - The total harmonic distortion of the alternator current is defined as the ratio of the rms value of all the harmonic frequency components of the function to the rms value of the fundamental component of the function (Ref. 5):

$$\text{Total harmonic distortion (THD)} = \frac{I_H}{I_{T1}} \tag{2}$$

The analysis evaluates Eq. (2) in terms of two parameters: (1) the power factor of the useful load and (2) the number of parallel parasitic-load resistors.

In terms of the rms (effective) value of the alternating current, the total harmonic distortion can be expressed as

$$\text{THD} = \frac{\left(I_T^2 - I_{T1}^2\right)^{1/2}}{I_{T1}} \tag{3}$$

Effective value of total current. - To obtain analytical expressions for I_T and I_{T1}, the instantaneous values i_T and i_{T1} are needed.

The total alternator current i_T is the sum of the useful-load current i_U, and the total parasitic-load current i_P. The parasitic-load current is further divided into two components: ni_{PR}, the current through n parasitic-load resistances which are fully on and i'_P, the current through the one parasitic-load resistance which is partially on. These currents are illustrated in Fig. 4.

$$i_T = i_U + (ni_{PR} + i'_P) \tag{4}$$

$$i_U = \sqrt{2}\, I_U \sin(\omega t - \theta_U) \tag{5}$$

$$i_{PR} = \sqrt{2}\, I_{PR} \sin \omega t \tag{6}$$

$$i'_P = 0 \Bigg|_{\frac{\alpha}{\omega},\, \frac{\alpha+\pi}{\omega}} \quad 0 \Bigg|_{\frac{\pi}{\omega}}$$

$$= \sqrt{2}\, I_{PR} \sin \omega t \Bigg|_{\frac{\alpha}{\omega},\, \frac{\alpha+\pi}{\omega}}^{\frac{\pi}{\omega},\, \frac{2\pi}{\omega}} \tag{7}$$

All the harmonics in the total current are introduced by i'_P.

Effective value of total current fundamental. - The fundamental component i_{T1} of the total current is composed of three signals:

$$i_{T1} = i_U + ni_{PR} + i'_{P1} \tag{8}$$

Fourier analysis (Ref. 1) of the waveform described by Eq. (7) yields the following expression for i'_{P1}:

$$i'_{P1} = \sqrt{2}\, I_{PR}\left(A^2 + B^2\right)^{1/2} \sin\, \omega t + \tan^{-1} \frac{A}{B} \tag{9}$$

where

$$A = \frac{\cos 2\alpha - 1}{2\pi} \tag{10}$$

$$B = 1 - \frac{\alpha}{\pi} + \frac{\sin 2\alpha}{2\pi} \tag{11}$$

The expressions for all the quantities involved in the analysis have been converted to a per unit system with the base quantities for power and voltage being rated alternator power, P_G, and rated voltage-source voltage, E_G. Because P_G and E_G are fixed quantities in this analysis, the corresponding per unit values are fixed at 1.

The effective values of i_T and i_{T1} in per unit form are

$$I_{Tpu} = \left\{\frac{1}{N^2}\left([NP_{Ppu}]^2 + 2[NP_{Ppu}]B + B\right) + \left(\frac{1 - P_{Ppu}}{\cos \theta_U}\right)^2 + \frac{2(1 - P_{Ppu})}{N \cos \theta_U}\left(NP_{Ppu} \cos \theta_U - A \sin \theta_U\right)\right\}^{1/2} \tag{12}$$

$$I_{T1pu} = \left\{\frac{1}{N^2}\left(N^2 P_{Ppu}^2 + A^2\right) + \left(\frac{1 - P_{Ppu}}{\cos \theta_U}\right)^2 + \frac{2(1 - P_{Ppu})}{N \cos \theta_U}\left(NP_{Ppu} \cos \theta_U - A \sin \theta_U\right)\right\}^{1/2} \tag{13}$$

Equations (12) and (13) are derived in detail in Ref. 1.

D. Total Harmonic Distortion of Mathematical Model

Two features of the variation of THD with parasitic loading are observable in the plots presented in Figs. 5 and 6 for lagging useful-load power factor loads.

(1) The peak THD is a function of the useful-load power factor.

(2) The peak THD is reduced by subdividing the total parasitic load into multiple phase-controlled parallel parasitic loads.

In Fig. 5 as power factor increases, the peak distortion is maximized. For the configuration of a single parasitic load (N = 1) the peak (worst case) value of THD occurs with a useful load of 1.0 power factor. Under these conditions the peak THD is 37 percent. The peak is reduced only to 30 percent for a 0.6 lagging power factor useful load. These figures show that the current distortion is appreciable over the range of practical power factor loads.

Figure 6 and Table I illustrate the effect on the harmonic content of using more than one parasitic loading unit. As the number of parallel loads increases, the maximum distortion is reduced. The greatest reduction occurs with the addition of a second parasitic-load resistor.

When there are two parallel parasitic loads, distortion varies with useful-load power factor in the same way as in the case of a single parasitic load shown in Fig. 5. In Fig. 6, the theoretical distortion for two parasitic loads goes to zero at 0.5 per unit. Likewise, for three parasitic loads, the distortion is zero at 0.33 and 0.67 per unit load. This is expected because there is no overlap in

the theoretical model and because the ideal switch is assumed capable of conducting for a full 180° per half cycle. The theoretical current in a fully on parasitic load is a sinusoid with zero distortion.

E. Analytical Expression for Apparent-Power

The parasitic load appears to the power source (the alternator) to be an inductive load. The inductive character is shown by the lagging phase angle between the reference voltage e_G and the fundamental component of the parasitic-load current i_{P1}. This current is the sum of the n fully on parasitic-load currents and the fundamental component of the one partially on parasitic load.

$$i_{P1} = i'_{P1} + n i_{PR} \tag{14}$$

Substitution of Eqs. (6) and (9) into Eq. (14) gives

$$i_{P1} = \sqrt{2}\, I_{PR}\left[A^2 + (B+n)^2\right]\sin\left(\omega t + \tan^{-1}\frac{A}{B+n}\right) \tag{15}$$

The phase angle $\tan^{-1} A/(B+n)$ is a negative for all values of α, so that i_{P1} always lags e_G.

Because the parasitic load is, in effect, a reactive load, it imposes an additional apparent-power (volt-ampere) capacity requirement on the source. Also the harmonic components of the current increase the necessary apparent-power capacity.

F. Apparent Power Requirements for Mathematical Model

Examination of Figs. 7 to 9 of apparent-power for lagging power-factor useful loads will indicate the significant features that

(1) The peak apparent-power increases as the useful-load power factor decreases from 1.

(2) There is a reduction in the apparent-power requirement when the total parasitic load is subdivided into multiple parasitic loads.

Point (1) is illustrated in Fig. 7 for a system with a lagging power factor useful load and a single parasitic load. As the useful-load power factor decreases, the maximum apparent-power requirement for the alternator increases.

In every case, as shown in Fig. 8, the peak apparent-power is greater than would be required for the useful load without the parasitic load. In fact, the ratio of the apparent-power requirement of the alternator with a parasitic load to the apparent-power requirement of that alternator without a parasitic load is particularly significant. This relative rating is the ratio

$$\text{Relative rating} = \frac{\text{Apparent-power requirement with parasitic load}}{\text{Apparent-power requirement without parasitic load}} \tag{16}$$

Relative ratings greater than 1 represent conditions for which the use of the parasitic load increases the apparent-power rating required of the alternator.

Figure 8 shows these relative values for the same loads as Fig. 7. A maximum ratio of 1.13 is reached when the power factor of the useful load is 0.98 lagging. This means that a 13 percent increase in apparent-power capacity is necessary when this useful load is used with a single parasitic load. A similar variation of relative apparent-power occurs with multiple parallel parasitic loads.

Figure 9 and Table II show how increasing the number of parallel parasitic loads reduces the magnitude of the relative rating ratio. As N increases, the maximum value of the ratio decreases, approaching a limiting value as N approaches infinity.

III. Description of Experimental System

The Brayton turboalternator used is a 12 000 rpm machine which operates on gas lubricated bearings. The alternator (Ref. 6) is a brushless, three-phase, 400 hertz, homopolar inductor. At design turbine inlet conditions the electrical output is approximately 9 kilowatts at 0.8 lagging power factor. A voltage regulator-exciter (Ref. 7) supplies excitation to the alternator field and regulates the voltage at the useful load. The parasitic speed controller (Ref. 8) uses silicon controlled rectifiers (SCR's) for power variation.

The breadboard speed controller tested consisted of 3 three-phase parasitic loads. The speed controller was tested in configurations using one, two, or three parasitic loads. In each case the sum of all parasitic loads fully on equaled the nominal turboalternator rating of 9 kilowatts. Thus, the operation of this Brayton power system was not performed under "design" conditions wherein the speed controller is overrated to improve dynamic response and to provide redundancy. A detailed description of the overall test apparatus used to obtain the experimental data is found in Ref. 9.

IV. Discussion of Experimental Results

A. Experimental Current Distortion

Theoretical and experimental values of alternator current distortion produced using one parasitic load, shown in Figs. 5 and 10 and Table III(a), demonstrate the reduction in peak distortion with decreasing useful load power factor.

In the experimental case, the distortion does not reduce to zero at zero parasitic load because of harmonics generated by the alternator. These harmonic components are small relative to those produced by the parasitic loading. Therefore, alternator distortion has its greatest relative effect at this point. The experimental curves also do not extend to 1 per unit parasitic load. This results from the maximum conduction restrictions which occur in real systems. One per unit parasitic load for these curves is the extrapolated value corresponding to 180° conduction per half cycle for the SCR's.

The most significant difference between the experimental and theoretical results lies in their relative magnitudes: The experimental values are significantly lower. This occurs despite the fact that the experimental alternator contributes to the distortion. The differences result from the presence of inductive reactances (principally the alternator reactance) in the experimental test circuit (Ref. 2) not considered in the mathematical analysis.

The variation of current distortion with the number of parallel parasitic loads is presented in Figs. 6 and 11 and Table III(b). The same general conclusion regarding lower experimental distortion drawn for one parasitic load can be made for the case of two parasitic loads. This is not always true for three parasitic loads. For a three parasitic load configuration, the peak experimental distortion of the alternator current is 3 percent higher than the theoretical value. This effect is caused by the overlap of parasitic operating ranges and by the limited conduction interval of the SCR's in the test circuit.

In the experimental case, the limited conduction range has a cumulative effect on the value of harmonic distortion. For the two load experimental case in Fig. 11, the minimum distortion for one load fully on is very nearly half the distortion for two loads fully on. In the same way for the three load case, the minimums for one load fully on and two loads fully on are about one-third and two-thirds, respectively, of the distortion occurring with three loads fully on. Thus each fully on parasitic load introduces a "residual" distortion. This residual distortion is not reduced by further action of additional parasitic loads.

At approximately 0.9 per unit parasitic load, each experimental combination of loads is at maximum conduction. The distortion is virtually the same in each case. Therefore, there exists a limit as to the extent to which maximum distortion of the alternator current can be reduced by increasing the number of parasitic loads. As a result, the effect of increasing the number of parasitic loads in order to reduce the overall harmonic distortion also becomes limited. This limitation results from the inability of experimental parasitic loads to conduct for a full 180° per half cycle. However, if the maximum SCR conduction interval can be increased by modification of the phase control circuitry, this limitation can be minimized.

B. Apparent-Power Requirements for Experimental System

Figures 7 and 12 present per unit alternator apparent-power as a

function of parasitic load for one speed control section. The peak values, which are shown in table IV, indicate only slight variations between the experimental and analytical cases. The peak values of the experimental curves are a measure of the minimum capacity for which the alternator must be rated in order to operate in this configuration.

Figures 8 and 13 show the alternator apparent-power required when using a single parasitic load relative to the apparent-power required without the parasitic load. Relative rating is defined by Eq. (16). This ratio is a measure of the necessary increase in alternator volt-ampere rating required when using phase-controlled parasitic loads. For example, consider the case of 0.8 lagging useful-load power factor. The peak apparent-power demand is 1.36 times the power output as shown in Table IV. For a linear load at 0.8 power factor, the apparent-power requirement is 1.25 times the real power. Thus, the ratio of peak apparent-power required using the parasitic load relative to the alternator apparent-power without the parasitic load is 1.36/1.25 or 1.08. A value greater than 1 indicates that the apparent-power demand occurring with the parasitic loading is greater than that for an equal but linear load. Peak values are tabulated in Table V(a).

The variation of relative apparent-power for one, two, and three parasitic loads at 0.8 lagging useful-load power factor is shown in Figs. 9 and 14. The peak values are summarized in Table V(b). The actual difference between the analytical and experimental results is, in each case, less than 1 percent.

V. Conclusion

The use of a phase-controlled parasitic current to maintain a constant power load on an alternator effects an increase in the apparent-power capacity required of the alternator. A phase-controlled current is nonsinusoidal. The current not only contains harmonics, but also, as generally used, is reactive. These features are responsible for the greater alternator capacity required.

Mathematical analysis of the circuit configuration assumed for the theoretical portion of this study showed that with a 0.8 lagging power factor useful load, the apparent-power (volt-ampere) rating of the alternator must be increased 7.6 percent above the rating required without a parasitic load. This theoretical result was confirmed experimentally. For the same useful load, the alternator relative apparent-power using one, two, or three parasitic loads in the experimental test system was within 1 percent of the theoretical value.

The size of the increase in alternator rating can be reduced by using more than one parasitic load. This analytic result was confirmed by the agreement of mathematical and experimental values for two and three parasitic loads. For the same 0.8 lagging power factor useful load, a second parasitic load used in parallel with the first reduces the required increase of the alternator capacity to 3.0 percent.

The generation of current harmonics predicted by the mathematical analysis of the phase-controlled currents is confirmed qualitatively by the experimental data. Quantitatively the experimental current harmonics were significantly less than the theoretical prediction for one and two parasitic loads. For a 0.8 lagging useful-load power factor, the experimental peak current distortion was lower by 24 percent of the theoretical value with one parasitic load and by 16 percent for two parasitic loads. These differences were caused by inductive reactances in the test circuits which were not considered in the analytical model.

Theoretically, the peak current distortion can be reduced with each increase in the number of parasitic loads. However, the peak distortion with three parasitic loads is higher for the test data than for the mathematical model. There is a limitation to the extent to which current distortion can be reduced by increasing the number of parasitic loads. This limitation is the result of restrictions in the conduction interval attainable in phase-controlled circuits.

Multiple smaller parasitic loads sequentially actuated reduce the undesirable effects of phase-controlled parasitic currents, but the amount of improvement at each division decreases rapidly with increasing number of loads.

List of Symbols

A	$\frac{\cos 2\alpha - 1}{2\pi}$
B	$1 - \frac{\alpha}{\pi} + \frac{\sin 2\alpha}{2\pi}$
E_G	rms value of source voltage
I_H	rms value of total harmonic current
I_{PR}	rms value of current in a single fully conducting parasitic load
I_T	rms value of total current
I_{Tpu}	per unit value of I_T
I_{T1}	rms value of fundamental component of total current
I_{T1pu}	per unit value of I_{T1}
I_U	rms value of useful-load current
i_P	instantaneous value of total parasitic-load current
i'_P	instantaneous value of current in partially conducting parasitic load
i_{PR}	instantaneous value of current in single fully conducting parasitic load
i_{P1}	instantaneous value of fundamental component of total parasitic-load current
i'_{P1}	instantaneous value of fundamental component of current in partially conducting parasitic load
i_T	instantaneous value of total current
i_{T1}	instantaneous value of fundamental component of total current
i_U	instantaneous value of useful-load current
N	total number of parasitic loads in parasitic-loading system
$[NP_{Ppu}]$	greatest integer in numerical value of product NP_{Ppu}
n	number of parallel parasitic loads turned on fully
P_G	average power provided by electrical source (alternator)
P_P	average power dissipated in total parasitic load
P_{Ppu}	per unit value of P_P
P_U	average power dissipated in useful load
R_P	resistance of each parasitic load resistor
R_U	useful load resistance
THD	total harmonic distortion
t	time
X_{LP}	apparent reactance produced by phase-controlled current of parasitic load
X_U	reactance of useful load
α	firing angle of phase-controlled current
θ_U	useful-load power factor angle
ω	angular frequency of source voltage

References

1. Gilbert, L. J., "Reduction of Apparent-Power Requirement of Phase-Controlled Parasitically Loaded Turboalternator by Multiple Parasitic Loads," TN D-4302, 1968, NASA, Cleveland, Ohio.

2. Perz, D. A. and Valgora, M. E., "Experimental Evaluation of Volt-Ampere Loading and Output Distortion for a Turboalternator with Multiple Load Phase-Controlled Parasitic Speed Controller," TN D-5603, 1969, NASA, Cleveland, Ohio.

3. Klann, J. L., "2 to 10 Kilowatt Solar or Radioisotope Brayton Power System," Intersociety Energy Conversion Engineering Conference, Vol. I, IEEE, New York, 1968, pp. 407-415.

4. Repas, D. S. and Valgora, M. E., "Voltage Distortion Effects of SNAP-8 Alternator Speed Controller and Alternator Performance Results," TN D-4037, 1967, NASA, Cleveland, Ohio.

5. Ryder, J. D., Electronic Fundamentals and Applications, 3rd ed., Prentice-Hall, Englewood Cliffs, N.J., 1964, p. 371.

6. Edkin, R. A., Valgora, M. E., and Perz, D. A., "Performance Characteristics of 15 kVA Homopolar Inductor Alternator for 400 Hz Brayton-Cycle Space-Power System," TN D-4698, 1968, NASA, Cleveland, Ohio.

7. Bollenbacher, G., Edkin, R. A., and Perz, D. A., "Experimental Evaluation of a Voltage Regulator-Exciter for a 15 Kilovolt-Ampere Brayton Cycle Alternator," TN D-4697, 1968, NASA, Cleveland, Ohio.

8. Word, J. L., Fischer, R. L. E., and Ingle, B. D., "Static Parasitic Speed Controller for Brayton-Cycle Turboalternator," TN D-4176, 1967, NASA, Cleveland, Ohio.

9. Wood, J. C., Valgora, M. E., Kruchowy, R., Curreri, J. S., Perz, D. A., and Tryon, H. B., "Preliminary Performance Characteristics of a Gas-Bearing Turboalternator," TM X-1820, 1969, NASA, Cleveland, Ohio.

TABLE I. - PEAK THEORETICAL TOTAL HARMONIC DISTORTION OF ALTERNATOR CURRENT

Useful-load power factor lagging	Number of parasitic loads, N				
	1	2	3	4	5
0.6	0.2954	0.1747	0.1224	0.0937	0.0757
.7	.3097	.1790	.1240	.0944	.0761
.8	.3236	.1825	.1253	.0950	.0764
.9	.3388	.1858	.1263	.0954	.0766
1.0	.3674	.1903	.1277	.0960	.0770

TABLE II. - PEAK THEORETICAL RELATIVE RATING

Useful-load power factor lagging	Number of parasitic loads, N				
	1	2	3	4	5
1.0	1.1181	1.0307	1.0138	1.0078	1.0050
.9837	[a]1.1308	------	------	------	------
.9	1.1091	1.0418	1.0248	1.0175	1.0133
.8	1.0762	1.0304	1.0186	1.0134	1.0101
.7	1.0489	1.0203	1.0125	1.0091	1.0072
.6	1.0290	1.0122	1.0080	1.0055	1.0038

[a]Worst case for N = 1.

TABLE III. - PEAK TOTAL HARMONIC DISTORTION OF ALTERNATOR CURRENT

(a) For single parasitic load

Useful load power factor lagging	Maximum distortion, percent	
	Experimental	Theoretical
1.0	--	37
.97	27	--
.8	25	32
.6	23	30

(b) For lagging useful load power factor, 0.8

Number of parasitic loads, N	Maximum distortion, percent	
	Experimental	Theoretical
1	25	32
2	15	18
3	16	13

TABLE IV. - PEAK APPARENT-POWER[a] REQUIRED OF ALTERNATOR WITH ONE PARASITIC LOAD

Useful load power factor lagging	Linear load only (theoretical)	Linear load plus parasitic load	
		Experimental	Theoretical
1.0	1.00	----	1.12
.97	1.03	1.17	----
.8	1.25	1.36	1.35
.6	1.67	1.68	1.72

[a]Normalized to total alternator power.

TABLE V. - PEAK EXPERIMENTAL RELATIVE RATING

(a) For one parasitic load

Useful load power factor lagging	Peak volt-amperes required	
	Experimental results	Theoretical results
1.0	----	1.12
.984	----	[a]1.131
.97	1.13	------
.96	----	1.10
.8	1.08	1.08
.6	1.01	1.03

(b) For lagging useful load power factor, 0.8

Number of parasitic loads, N	Peak volt-amperes required	
	Experimental results	Theoretical results
1	1.08	1.08
2	1.03	1.03
3	1.02	1.02

[a]Peak theoretical value.

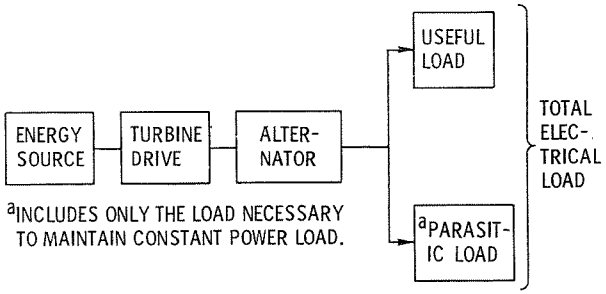

Figure 1. - Turboalternator system with parasitic loading.

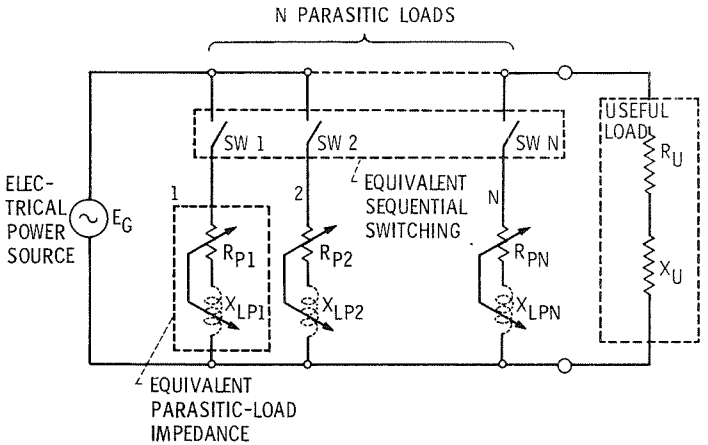

Figure 2. - Schematic diagram of ac model voltage source with multiple parasitic loads.

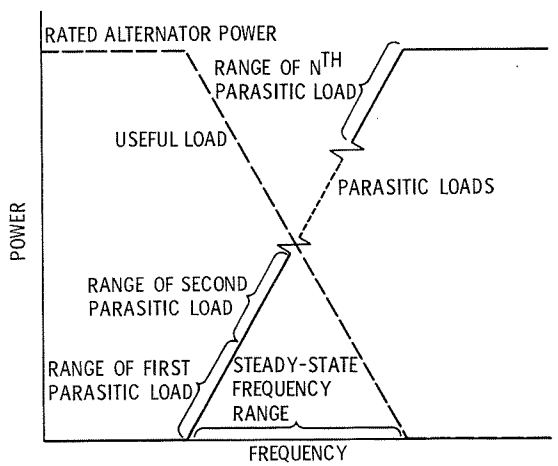

Figure 3. - Schematic diagram of ideal load distribution of parasitically loaded alternator for N parallel parasitic loads.

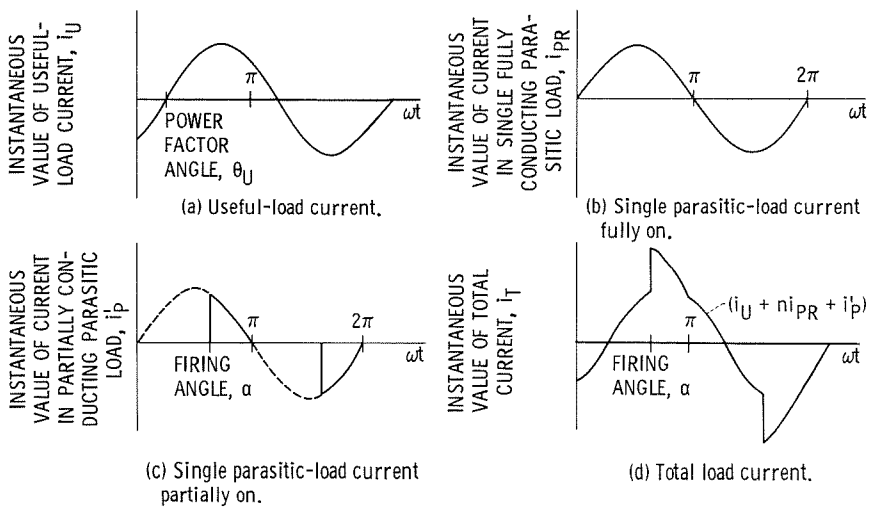

Figure 4. - Load currents for alternator with phase controlled parasitic load (not to scale).

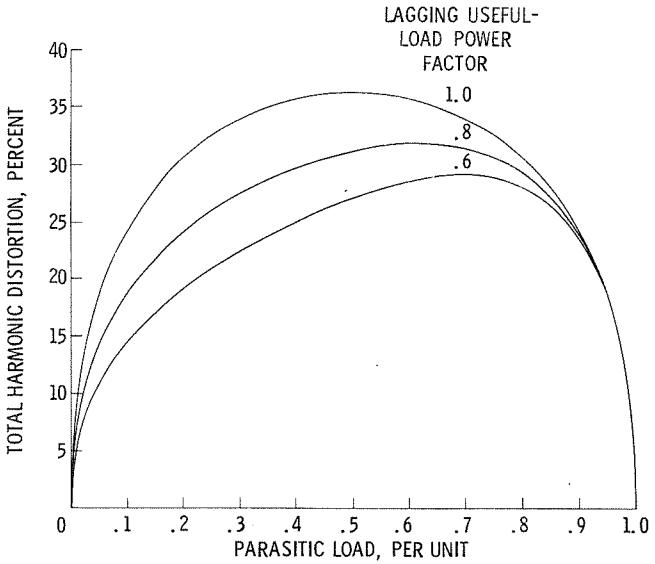

Figure 5. - Theoretical alternator current distortion for one parasitic load.

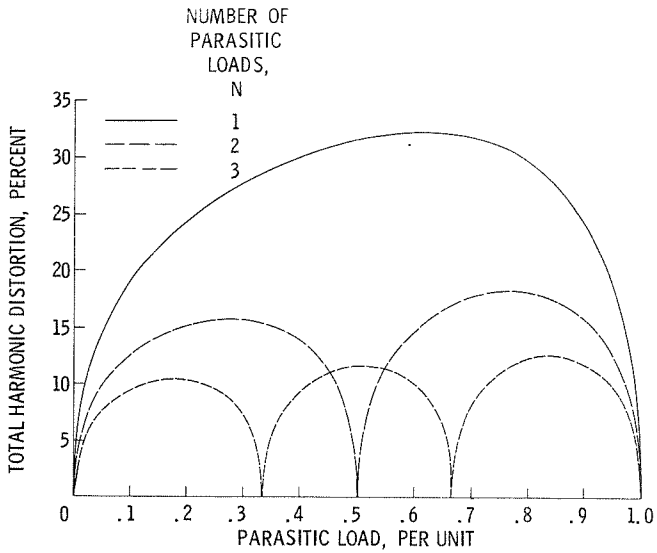

Figure 6. - Theoretical alternator current distortion for N parallel parasitic loads. Lagging useful load power factor, 0.8.

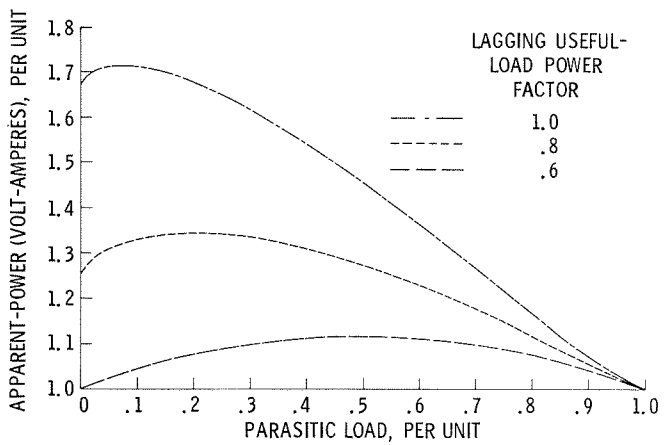

Figure 7. - Theoretical alternator apparent-power for one parasitic load.

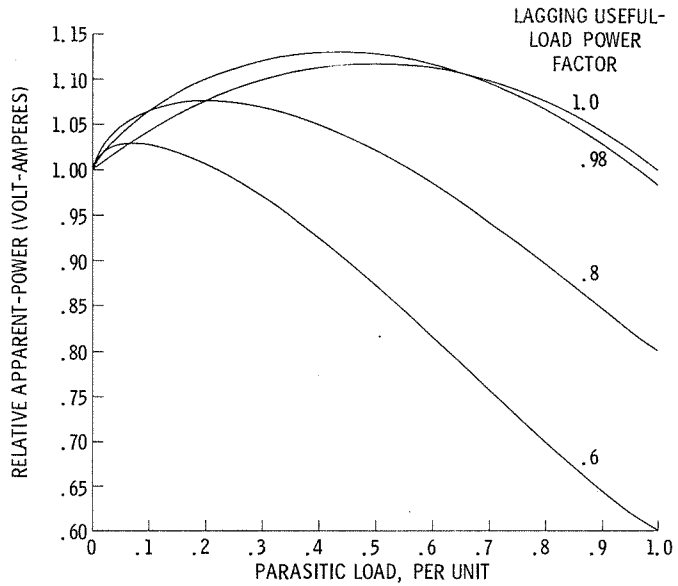

Figure 8. - Theoretical alternator relative apparent-power using one parasitic load.

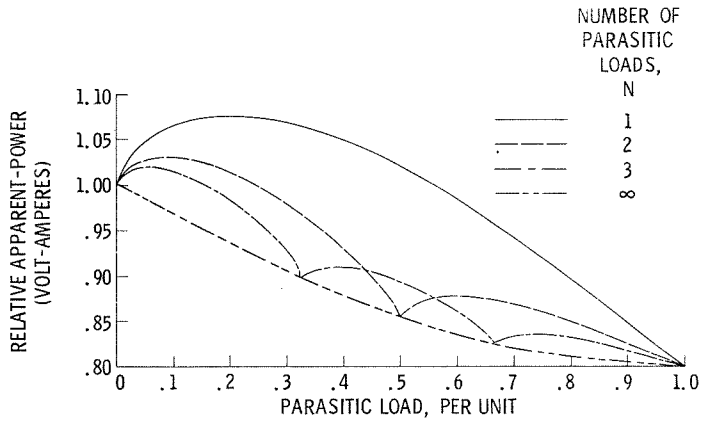

Figure 9. - Theoretical alternator relative apparent-power required with N parallel parasitic loads. Lagging useful load power factor, 0.8.

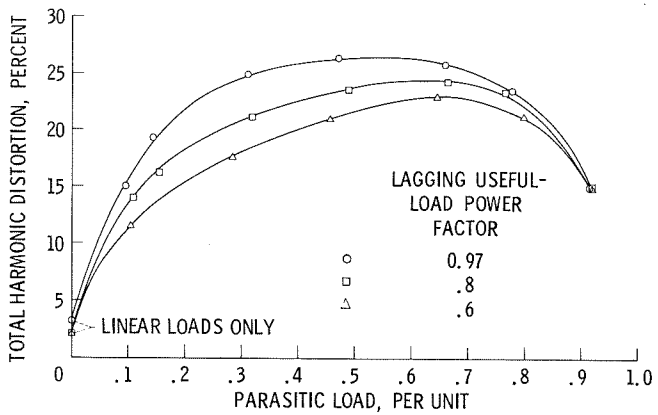

Figure 10. - Experimental alternator current distortion for one parasitic load.

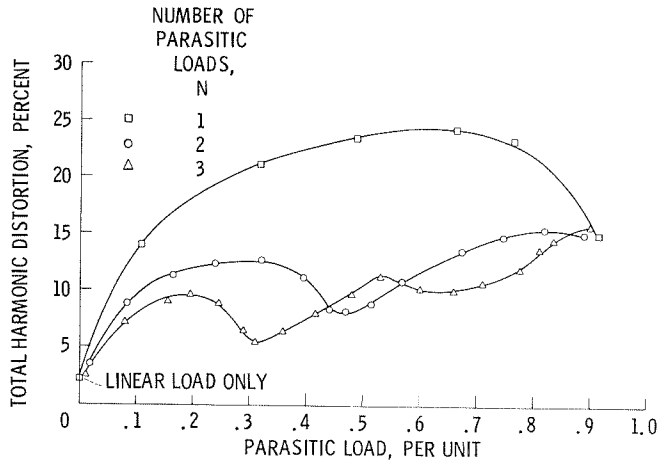

Figure 11. - Experimental alternator current distortion for N parallel parasitic loads. Lagging useful load power factor, 0.8.

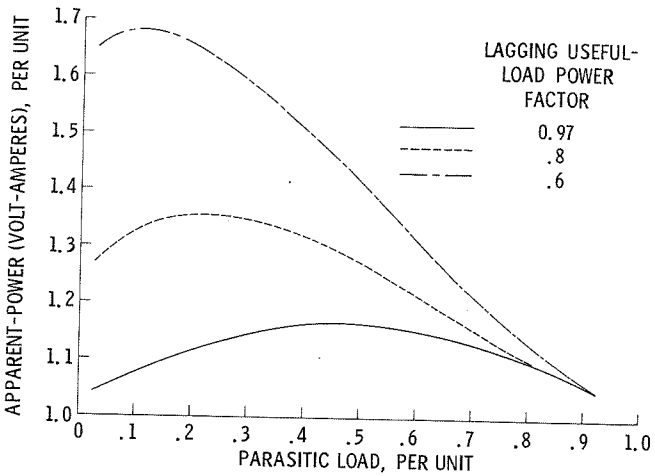

Figure 12. - Experimental apparent-power for one parasitic load.

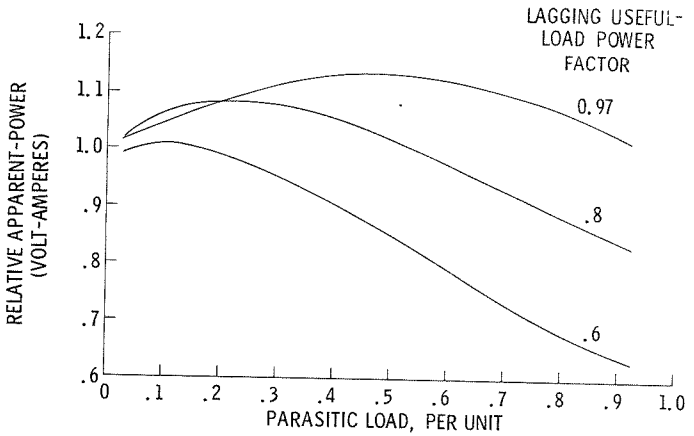

Figure 13. - Experimental alternator relative apparent-power for one parasitic load.

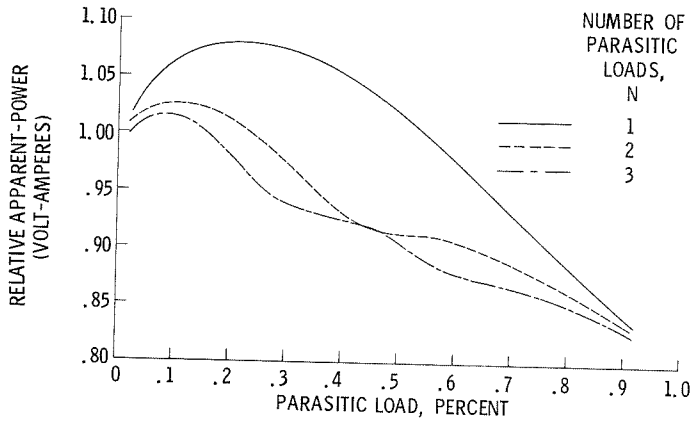

Figure 14. - Experimental alternator relative apparent-power for N parallel parasitic loads. Lagging useful load power factor, 0.8.